**Faculty of Engineering & Technology**
**Electrical & Computer Engineering Department**

# Electrical Machines Laboratory (ENEE3101)

## Report 2

**"Separate Winding "SW" Squirrel Cage Motor"**

---


**Prepared by:**

Eman Asfour 1200206

**Partners:**

Sadeel Ali 1200487

Omar Bader 1201443

**Instructor**: Dr.Ali Abdo

**Assistant**: Eng.Rafah Rahhal


8/10

-1 for being late.

**Section:** 1

**Date:** 27/12/2023

# Table of Contents



0.5

# 1. Abstract

Operating a changeable-pole, three-phase induction motor with different windings for slow and fast speeds involves connecting it to a pole-changer. This setup lets the motor adapt to various speed needs. Using the winding for slow speeds, which has more poles, makes the motor work well for gradual movements. On the other hand, using the winding for fast speeds, with fewer poles, smoothly switches the motor to faster rotations. In the experiment, careful recording and understanding of things like power use, efficiency, and torque give us a good picture of how the motor behaves at different speeds. This detailed look helps us adjust the motor for specific uses, ensuring we control speed precisely and use energy efficiently.

# 2. Method used

| | |
|---|---|
| **1 "SW" squirrel cage motor** | **732 26** |
| **1 machine test system** | **731989** |
| **1 CBM 10 computer-based analysis of electrical machines, V.5** | **728421** |
| **1 three-phase supply unit with FCCB** | **726 75** |
| **1 motor protection switch, 1 ... 1.6 A** | **732 14** |
| **2 RMS meters** | **727 10** |
| **1 power factor meter** | **727 12** |
| **1 power circuit breaker module** | **745 561** |
| **1 motor protection switch 1 ... 1.6 A** | **732 14** |
| **1 pole-changer, separate windings** | **731 57** |

*Table 1: The method of used in experiment*

0.5

# Table of figures

# Table of tables

# Table of Equations

# 3. Theory

### Asynchronous motor

The kind of motor chosen depends on how the rotor interacts with the rotating magnetic field. Take the Asynchronous Motor, for example; it runs with an alternating magnetic field, creating a current in the rotor. It's crucial to note that the rotor and stator aren't synchronized in design. The stator's rotating winding produces a magnetic field in the rotor, generating a force that moves the rotor towards the stator. Because the rotor isn't synchronized with the stator, it creates torque, highlighting the motor's functionality. In an asynchronous motor, you can configure the rotor as a squirrel cage or a slip ring, each design catering to specific performance needs. On the flip side, the stator is connected to the three outer conductors of a 3-phase system. When activated, the stator generates a rotating magnetic field at a synchronous speed (ns), determined by the number of poles (P) and electrical frequency (fe).

$$n_s = \frac{120 f_e}{P}$$

*Equation 1:speed calculation formula*

An asynchronous motor's rotor actually rotates at a speed called the mechanical speed (n), which is lower than the synchronous speed. Slip (s) is the difference between mechanical and synchronous speed. The motor's operating characteristics can be fine-tuned to meet specific requirements by adjusting the slip.

$$n = (1 - 2) n_s$$

*Equation 2: Mechanical speed formula*

Where s is the slip and giving by

$$s = \frac{\mathrm{n}_s - n}{\mathrm{n}_s}$$

*Equation 3: Slip formula*

It is simple to change the direction of rotation of an asynchronous motor. The motor's rotation can be changed by simply switching the stator connections for two input power phases, which essentially reverses the direction of the rotating magnetic field.

Certain formulas are needed to calculate the mechanical output power of electrical machines, such as asynchronous motors. One useful tool for understanding and forecasting the motor's performance under nominal operating conditions is Equation 4, which computes the nominal torque (TN) when the motor runs at its rated speed and power.

$$P_N = \omega_N * t_N$$

*Equation 4: Nominal Power formula*

The absence of an external exciter is the primary difference between the operation of synchronous motors and asynchronous motors, commonly referred to as induction motors. Unlike DC motors, these motors run on the electromagnetic induction principle, which prevents the rotor from obtaining electricity through conduction. Asynchronous motors rely on varying magnetic induction to drive their rotor speed instead of external stimuli. These motors are referred to as asynchronous when the rotor rotates slower than the magnetic field of the stator. Slip is the name given to this variation in speed**.**

### Power Losses and Power-Flow Diagram

An Induction motor can be likened to a rotating transformer with a short-circuited secondary winding. In this configuration, there is no electrical output power; rather, the resulting power is in the form of mechanical energy. Thus, the power flow diagram of an Induction motor can be depicted as follows

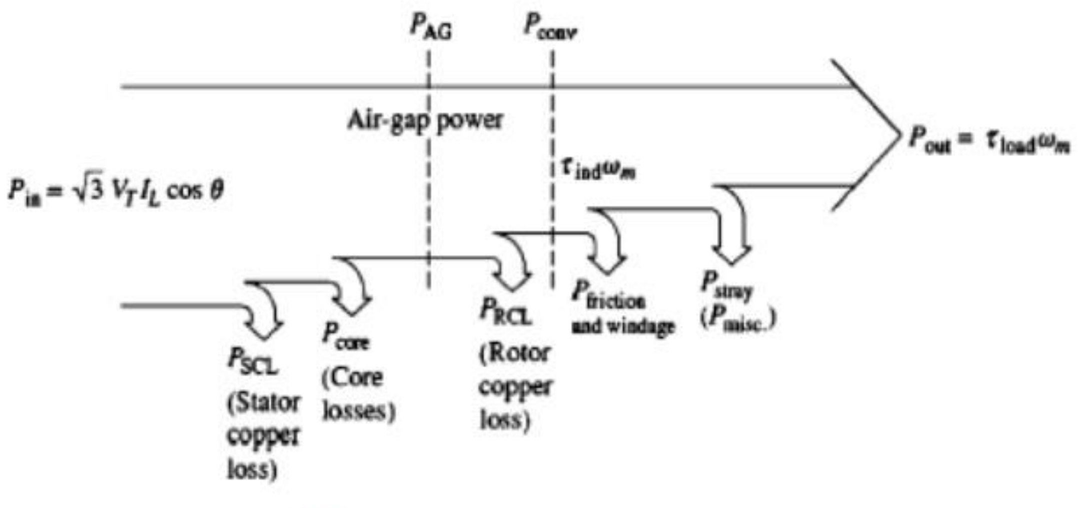


*Figure 1: Power-Flow Diagram*

$$P_{in} = \sqrt{3} * V_T * I_L * cos\theta$$

*Equation 5: Power input*

$$P_{out} = \tau_{load} * \omega_m$$

*Equation 6: Power output*

The losses in the core emanate partly from both the stator and rotor circuits, although the predominant share is attributed to the stator circuit. If the core power losses are quantified as a specific value (X Watts), they are combined with or aggregated into the mechanical losses. The rotational losses encompass factors such as friction, windage, and stray losses. [1]

**The control of speed in induction motors**

Can be achieved through various methods, including:

1. Pole Changing:

This technique involves altering the number of poles through a straightforward switching operation, typically with a ratio of 2:1.

- Implementation is uncomplicated in Squirrel-Cage motors, while in Wound-Rotor motors, rearranging the rotor windings is necessary.

The speed adjustment achieved through this method is by a factor of 2:1.

2. Changing the Rotor Resistance:

Adjusting the resistance in the rotor circuit provides a means of controlling the motor speed.

3. Changing the Line Voltage

Variation in the line voltage supplied to the motor impacts its speed.

4. Changing the Line Frequency:

Manipulating the line frequency is another effective means of regulating the speed of induction motors.

5. Variable Voltage Variable Frequency Drives (VVVF):

This modern method employs drives that allow independent control of both voltage and frequency, providing a highly versatile approach to speed regulation.

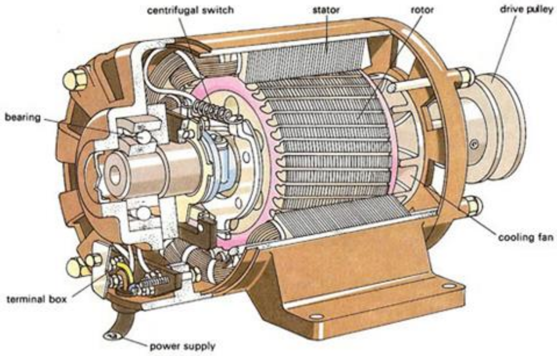


*Figure 2: Three Phase Induction Motors [2]*

### Example for application low speed three-phase induction motors

Three-phase induction motors with low-speed requirements are commonly used in specific applications where a slower rotational speed is necessary. Here are some examples:

1. Gear Motors for Conveyors:

In material handling systems, conveyors often require low-speed operation for precise movement and control. Three-phase induction motors, coupled with gear mechanisms, can provide the necessary torque at lower speeds.

2. Slow-Speed Pumps and Mixers:

Some industrial processes, such as in chemical and pharmaceutical industries, require pumps and mixers to operate at low speeds for accurate dosing and mixing. Three-phase induction motors with speed control mechanisms are employed for such applications.

3. Extruders in Manufacturing:

In the plastics and rubber industries, extruders used for shaping materials often require low-speed operation. Three-phase induction motors with variable frequency drives (VFDs) allow precise control of the extruder speed.

4. Slow-Speed Fans for Ventilation:

In ventilation and HVAC systems, slow-speed fans may be required for applications where a constant, low airflow is needed. Three-phase induction motors can be designed or controlled to operate efficiently at lower speeds.

5. Slow-Speed Grinders and Crushers:

Certain industrial processes, such as in mining and material processing, may require slow-speed grinders or crushers for efficient size reduction. Three-phase induction motors can be tailored for such applications.

6. Slow-Speed Agitators in Chemical Processing:

Chemical processing often involves the use of slow-speed agitators for mixing and reacting substances. Three-phase induction motors with speed control capabilities can be employed in these applications. [3]

### Example for application High speed three-phase induction motors

Three-phase induction motors are also widely used in applications that require high-speed operation. Here are some examples:

- Centrifugal Pumps and Fans:

High-speed centrifugal pumps and fans are often used in HVAC systems, industrial processes, and water supply systems. Three-phase induction motors can drive these applications efficiently at high speeds.

- High-Speed Spindles in Machine Tools:

Machine tools, such as milling machines and lathes, often require high-speed spindles for precision machining. Three-phase induction motors, especially those designed for high-speed applications, are employed in these scenarios.

- Compressors in Air Compression Systems:

Certain industrial applications, such as air compression systems in manufacturing plants, may require high-speed compressors. Three-phase induction motors can be adapted for these high-speed requirements.

- High-Speed Conveyors:

Industries with high-speed material handling requirements, such as packaging and logistics, may utilize high-speed conveyors. Three-phase induction motors can efficiently drive conveyor systems at elevated speeds.

- Electric Vehicles with High-Speed Requirements:

Some electric vehicles, particularly those designed for highway use, may employ high-speed three-phase induction motors for efficient and powerful propulsion.

High-Speed Blowers:

Industrial processes, such as those in the petrochemical and chemical industries, may use high-speed blowers for material handling and processing. Three-phase induction motors can drive these blowers at high speeds.

7. Low-Speed Electric Vehicles:

Some electric vehicles, especially those designed for specific applications such as industrial carts or warehouse vehicles, may utilize low-speed three-phase induction motors for propulsion.

8. Winders and Tension Control Systems:

In industries like textile manufacturing, winding and tension control systems may require low-speed operation for precise control of material winding. Three-phase induction motors can be used in such systems.

9. Low-Speed Compressors:

Certain applications, such as in specialized compressors, may require low-speed operation. Three-phase induction motors with the appropriate design or control mechanisms can meet these requirements. [4]

Low-speed squirrel cage induction motors are designed to operate efficiently at reduced rotational speeds, making them suitable for applications requiring precise control and torque at lower velocities. These motors find utility in scenarios such as conveyor systems, mixers, and pumps where a steady, controlled movement is essential. They often incorporate features like gear mechanisms or variable frequency drives (VFDs) to achieve optimal performance at lower speeds.

Conversely, high-speed squirrel cage induction motors are engineered to deliver robust performance at elevated rotational speeds. These motors are well-suited for applications demanding rapid and efficient operation, such as high-speed spindles in machine tools, blowers in industrial processes, and certain types of compressors. Their construction and design considerations prioritize the ability to handle the mechanical stresses associated with higher speeds, ensuring reliability and effectiveness in demanding high-speed applications. [5]

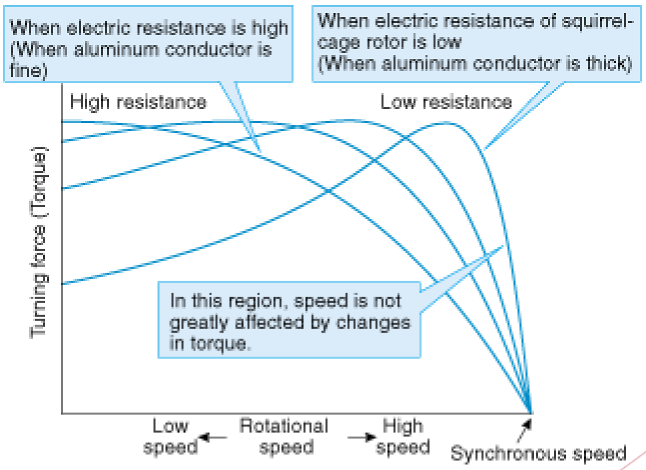


*Figure 3: Characteristics of Induction Motors [6]*

1.5

## 4. Procedure, Data and Calculations

### i. Basic Circuit

In Figure 4, the circuit was set up, and subsequently, activation was initiated for all models. Following verification by our supervising doctor, the power button on the circuit breaker was engaged. Subsequently, measurements of current in one phase, line-to-line voltage, speed, and its directional aspect were conducted and recorded in Table 2. Finally, deactivation of the machine test system was performed by pressing the OFF button, effectively isolating the power from the machine.

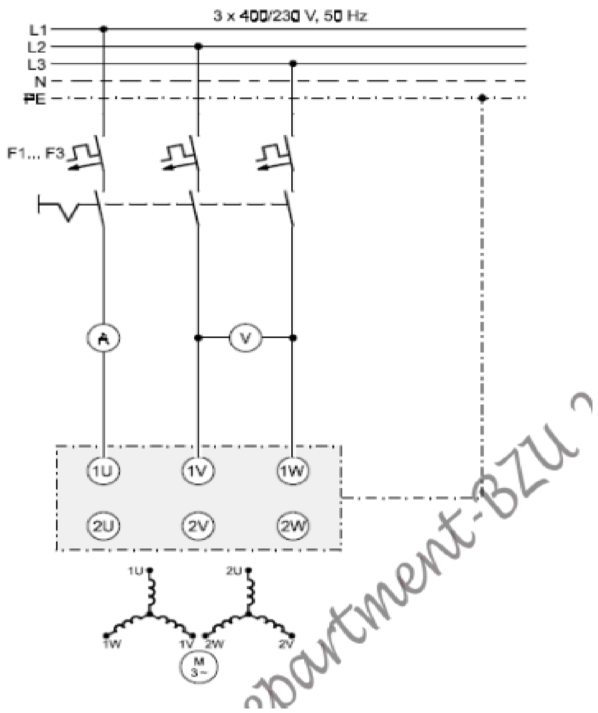


*Figure 4: Circuit for studying the behavior of SW squirrel cage induction motor*

| Quantity | Measured Value |
|---|---|
| **$I_{phase}$** | **0.45A** |
| **$V_{line-line}$** | **400V** |
| **Speed** | **994rpm** |
| **Direction** | **Counterclockwise** |

*Table 2: SW squirrel cage induction motor - low speed mode*

Figure 5 was adopted for the circuit modification, and subsequently, activation for all models was initiated. Following the activation, the power circuit breaker modules ON button was pressed, supplying power to the machine under the supervision of the doctor. Subsequently, measurements of current in one phase, line-to-line voltage, speed, and directional aspects were conducted and recorded in Table3. Finally, deactivation of the machine test system was executed by pressing the OFF button, effectively isolating the power from the machine.

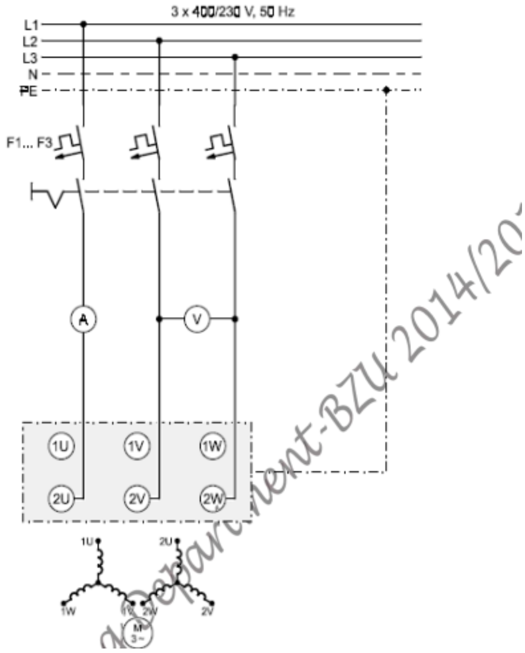



*Figure 5: Circuit for studying the behavior of SW squirrel cage induction motor*

| Quantity | Measured Value |
|---|---|
| **I** $_{phase}$ | **0.67A** |
| **V** $_{line - line}$ | **400** |
| **Speed** | **1494** |
| **Direction** | **Counter wise** |

*Table 3: SW squirrel cage induction motor - high speed mode*

The motor speed in Table 3 (High Speed Mode, 1494rpm) is higher than that in Table 2 (Low Speed Mode, 994rpm).The change in speed when switching from low speed mode (Table 1) to high speed mode (Table 2) is likely due to a change in the number of poles. The squirrel cage induction motor in the "High Speed Mode" (corresponding to Table 2) has a higher speed compared to the "Low Speed Mode" (corresponding to Table 1). The change in speed is likely due to a change in the number of poles, with the high-speed mode having fewer poles, resulting in a higher speed of operation. The exact number of poles would need to be determined from additional information or motor specifications.

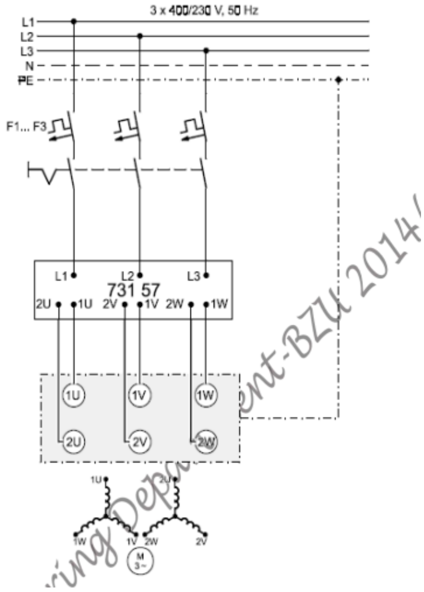


*Figure 6: The usage of a pole-changer to change the speed of rotation*

The circuit was connected as illustrated in Figure 6. Subsequently, the ON button of the power circuit breaker module was pressed under the supervision of the doctor. The functionality of the power circuit breaker module was tested by transitioning its position from 0 to 1 to 2. Finally, the OFF button of the power circuit breaker module was pressed.

### ii. Determining Efficiency and Recording Characteristics in Motor Operation

#### i. Efficiency Calculations

The data printed on the machine's nameplate was utilized to populate Table 4. Subsequently, the circuit was connected according to the configuration depicted in Figure 7. The Nominal Torque (TN) was then calculated using the data from Table 4. The pole-changer switch was set to the low-speed position (position 1), and the ON button of the power circuit breaker module was pressed. Under the operation mode, the "torque control mode" was selected, followed by pressing OK. This mode permits the control of the load torque on the machine. The RED button of the machine test system was pressed, and the calculated nominal torque value was set as a load for the machine. The load torque was adjusted slightly until the output power of the machine approached the recorded nominal value, establishing the machine at its nominal point. Measurements were then taken, including the line-to-line voltage (VL-L), current in one phase, power factor $Cos(\theta)$, speed of rotation, and load torque. Subsequently, the motor was unloaded by pressing the red button on the machine test system. Furthermore, the pole-changer switch was set to the high-speed position, and finally, the off button of the power circuit breaker module was pressed.

| | |
|---|---|
| Nominal Voltage $V_N$ | **400** |
| Nominal current $I_N$ (low speed) | **0.6** |
| Nominal Current $I_N$ (high speed) | **0.7** |
| Nominal Power Factor, $Cos(\theta_N)$ (low speed) | **0.7** |
| Nominal Power Factor, $Cos(\theta_N)$ (high speed) | **0.72** |
| Nominal speed $n_N$ (low speed) | **880** |
| Nominal speed $n_N$ (high speed) | **1390** |
| Nominal Power $P_N$ (low speed) | **0.11K** |
| Nominal Power $P_N$ (high speed) | **0.20KW** |

*Table 4: Nominal data for the machine under test*

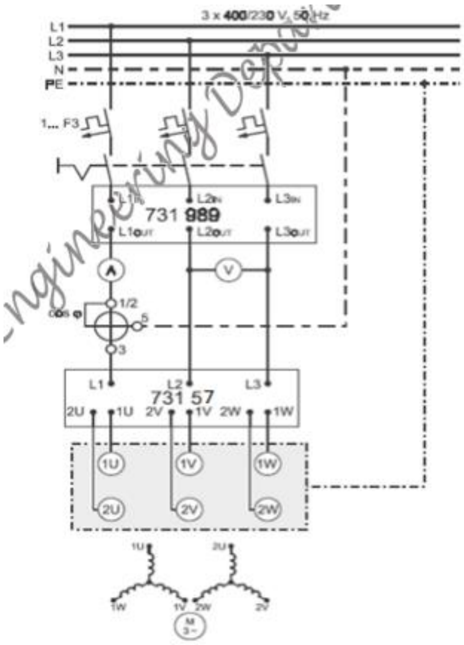


*Figure 7: Circuit for studying the SW squirrel cage induction motor*

Given the provided nominal values in the table above, the calculation of the nominal torque $\tau_N$ is straightforward.

- ❖ Low speed mode

$$P_N = \omega_N * \tau_N$$

$$\tau_N = \frac{60}{2\pi} \frac{P_N}{\omega_N}$$

*Equation 7: The Torque equation*

$$\tau_N = \frac{60}{2\pi} \frac{0.11k}{880} = 1.194\text{Nm}$$

The calculation of the input power can be performed by:

$$P_{in} = \sqrt{3} V_L \, I_L \, cos\theta$$

$$P_{in} = \sqrt{3}\, 400\ 0.6\ 0.7 = 290.98\ \text{W}$$

The theoretical efficiency can be determined by:

$$\eta = \frac{P_{out}}{P_{in}} \times 100\%$$

$$\eta = \frac{0.11k}{290.98} \times 100\% = 37.80\%$$

- High speed mode :

Given the provided nominal values in the table above, the calculation of the nominal torque $\tau_N$ is straightforward.

- Low speed mode

$$P_N = \tau_N \, \omega_N$$

$$\tau_N = \frac{60}{2\pi} \frac{P_N}{\omega_N}$$

$$\tau_N = \frac{60}{2\pi} \frac{0.20k}{1390} = 1.373\text{Nm}$$

The calculation of the input power can be performed by:

$$P_{in} = \sqrt{3} V_L \, I_L \, cos\theta$$

$$P_{in} = \sqrt{3}\, 400\ 0.7\ 0.72 = 349.181\ \text{W}$$

The theoretical efficiency can be determined by:

$$\eta = \frac{P_{out}}{P_{in}} \times 100\%$$

$$\eta = \frac{0.20k}{349.18} \times 100\% = 57.27\%$$

In comparing the performance of the squirrel cage motor in both low-speed and high-speed modes, certain key observations can be made. In the low-speed mode, the motor exhibits a nominal torque

($\tau_N$) of 1.194 Nm, with an input power ($P_{in}$ ) of 290.98 W, resulting in a theoretical efficiency ($\eta$) of 37.80%. Transitioning to the high-speed mode, the nominal torque ($\tau_N$) increases to 1.373 Nm, accompanied by an input power ($P_{in}$ ) of 349.181 W and a higher theoretical efficiency ($\eta$) of 57.27%. This comparison highlights the motor's ability to generate higher torque and efficiency at high-speed mode, demonstrating its adaptability and performance across different operational conditions.

### ii. Load Characteristics

The Load Characteristics, defining the relationship between current, power factor, and related values concerning load torque, were studied in this section. The behavior of the machine under test was analyzed for various load torque values. For the measurements presented, the normalized values for readings (I, V, Cos(θ), etc.) were calculated using the nominal values obtained in steps 7 and 8 from the preceding section, filling the T/[Nm] rows in Table 5. Subsequently, the low-speed position of the pole-changer was set (position 1). The ON button of the power circuit breaker module was pressed under the supervision of our doctor. Synchronization of the machine test system with the motor was initiated by the pressing of the red button, ensuring that the system was in Torque control mode. Following the setup, torque was incrementally increased in steps, as outlined in Table 5. For each torque value, the red button on the machine test system was pressed. The OFF button of the power circuit breaker module was then pressed to conclude each step in the analysis.

$$\tau_N = \frac{P_N}{\omega_N} = \frac{110}{\frac{2\pi}{60} * 880} = 1.19$$

| **T/T$_{N,act}$** | **0** | **0.2** | **0.4** | **0.6** | **0.8** | **1** |
|---|---|---|---|---|---|---|
| **T/[Nm]** | 0 | 0.238 | 0.476 | 0.714 | 0.952 | 1.19 |
| **n/[rpm]** | 1015 | 988 | 975 | 960 | 940 | 925 |
| **I/[A]** | 0.7 | 0.63 | 0.639 | 0.61 | 0.66 | 0.68 |
| **cos(ϑ)** | 0.2 | 0.35 | 0.45 | 0.5 | 0.6 | 0.64 |
| **n/Nn** | 1.153409 | 1.122727 | 1.107954 | 1.090909 | 1.068181 | 1.059091 |
| **I/I$_{N,act}$** | 1.166666 | 1.05 | 1.065 | 1.016666 | 1.1 | 1.1 |
| **P1/[W]** | 96.9948 | 152.7668 | 199.220 | 211.3102 | 290.9845 | 301.5154 |
| **p1/p1N** | 0.881409 | 1.81393 | 1.81393 | 1.921001 | 2.645313 | 2.701999 |
| **P2/[W]** | 0 | 24.62422 | 48.60043 | 71.77911 | 93.71161 | 115.2702 |
| **p2/p2N** | 0 | 0.123212 | 0.243002 | 0.358896 | 0.468558 | 1.055842 |

| ŋ | 0 | 16.11882 | 24.39535 | 33.96859 | 34.15683 | 38.2303 |
|---|---|---|---|---|---|---|

*Table 5: Measurement for Load Characteristic recording for the SW squirrel cage in low speed mode*

$$P_1 = \sqrt{3}\, 400\ 0.7\ 0.2 = 96.994\ \text{W}$$

$$P_2 = \tau * \omega = 0.238 * \frac{2 * \pi * n(988)}{60} = 24.62422$$

$$\frac{n}{N_n} = \frac{985}{880} = 1.1193$$

$$\eta = \frac{P_2}{P_1} * 100\% = 16.11$$

| **T/T$_{N,act}$** | **0** | **0.2** | **0.4** | **0.6** | **0.8** | **1** |
|---|---|---|---|---|---|---|
| **T/[Nm]** | 0 | 0.274 | 0.548 | 0.822 | 1.096 | 1.37 |
| **n/[rpm]** | 1498 | 1485 | 1472 | 1457 | 1442 | 1420 |
| **I/[A]** | 0.65 | 0.66 | 0.65 | 0.67 | 0.69 | 0.699 |
| **cos(ϑ)** | 0.2 | 0.23 | 0.4 | 0.5 | 0.6 | 0.7 |
| **n/Nn** | 1.077697 | 1.068345 | 1.058992 | 1.0482014 | 1.037410 | 1.021583 |
| **I/I$_{N,act}$** | 0.928571 | 0.942857 | 0.928571 | 0.9571428 | 0.985714 | 0.998571 |
| **P1/[W]** | 90.06664 | 105.1701 | 180.1332 | 232.0948 | 286.8276 | 338.9969 |
| **p1/p1N** | 0.45233 | 0.525851 | 0.675499 | 1.1604740 | 1.434138 | 1.808653 |
| **P2/[W]** | 0 | 42.60942 | 84.47281 | 125.41803 | 165.5024 | 205.1564 |
| **p2/p2N** | 0 | 0.213047 | 0.422364 | 0.6270901 | 0.827512 | 1.025782 |
| **ŋ** | 0 | 40.51476 | 46.89463 | 50.5264 | 57.70102 | 60.51865 |

*Table 6: Measurement for Load Characteristic recording for the SW squirrel cage in high speed mode*

$$\tau_N = \frac{P_N}{\omega_N} = \frac{200}{\frac{2\pi}{60} * 1390} = 1.374$$

### iii. Computer-based Recording of Run-up Characteristics

The plotting of curves representing the motor's behavior was facilitated using the computer, first during high-speed operation and subsequently during low-speed operation. The CBM 10 software was opened by navigating to Start >> All Programs >> CBM10 >> MOMO.exe, and MOMO was clicked on to initiate the software opening. The machine under test type was chosen by selecting "Squirrel Cage Induction Motor 400/690V" under Machine Type in the toolbar, and the Torque Y axis was displayed by clicking on T from the left-side column. The axis settings were adjusted via Presentations >> Axis scaling. Initially, all nominal value boxes were checked, and the Nominal Values fields were filled with the values obtained for the machine in this experiment. The Y axis values for parameters were then modified according to the limits specified in Table 7, which outlined Y-axis limits for plotting parameters like speed (n) and torque. Position 2 (the high-speed position) was set for the pole changer. The motor was powered on by pressing the ON button of the 745 561 module. In the CBM 10 software, the synchronization button, located in the left-hand column and functioning as the Green button, was pressed to synchronize the machine test system with the motor. Automated Mode recording was chosen, and in Measurements >> Settings, the motor operation box was checked, the operational mode was set to Load Characteristics, the start-up speed was set to 1490 rpm, and the stop speed was set to 50 rpm. Plotting was initiated by pressing the RUN button on the software (the blue arrow in the upper left corner). Upon completion, the machine test system was isolated from the motor by pressing the RED button on the software. Subsequently, the OFF button of the power circuit breaker module was pressed, and the pole changer was adjusted to the low-speed position (position 1).

| Parameter | From | To |
|---|---|---|
| **n** | 0 | 1.2 |
| **torque** | 0 | 2.5 |

*Table 7:Y axis limits for the stated parameter for plotting*

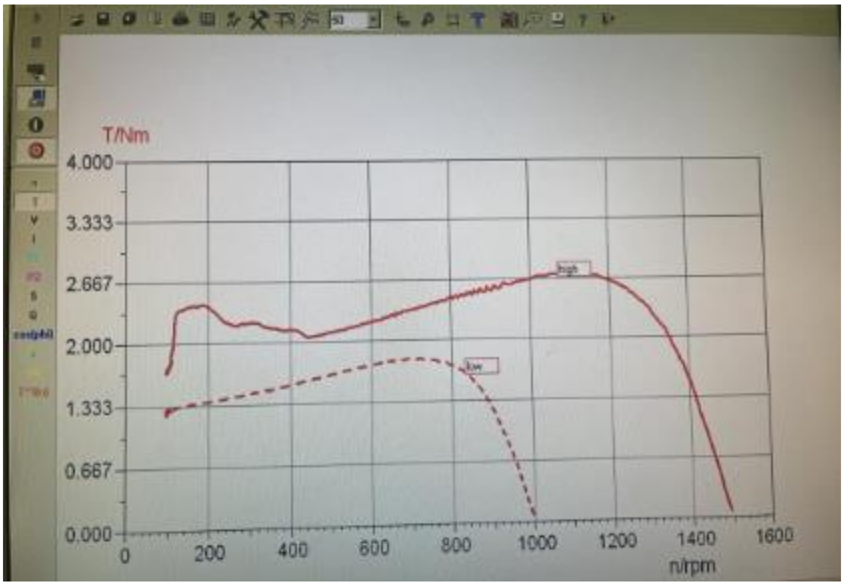


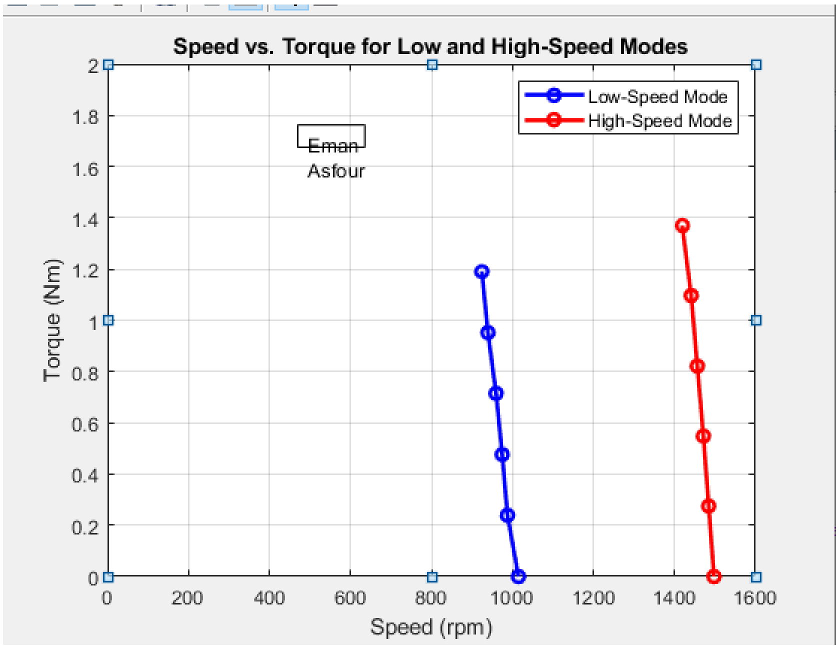


The figure unequivocally depicts a pronounced inverse correlation between torque and speed in both high and low operational modes of the machine. As torque undergoes an increment, speed consistently registers a decrement, irrespective of the operational range. This underlines the inherent and crucial interdependence of these parameters in influencing the machine's performance, affirming its capability to generate more power at lower speeds. Notably, while the high-speed mode boasts slightly faster operation, it does so at the expense of some torque compared to the low-speed mode. These keen insights illuminate a discernible trade-off between torque and speed, presenting valuable information that can be leveraged for a comprehensive understanding and optimization of the machine's performance across diverse load conditions

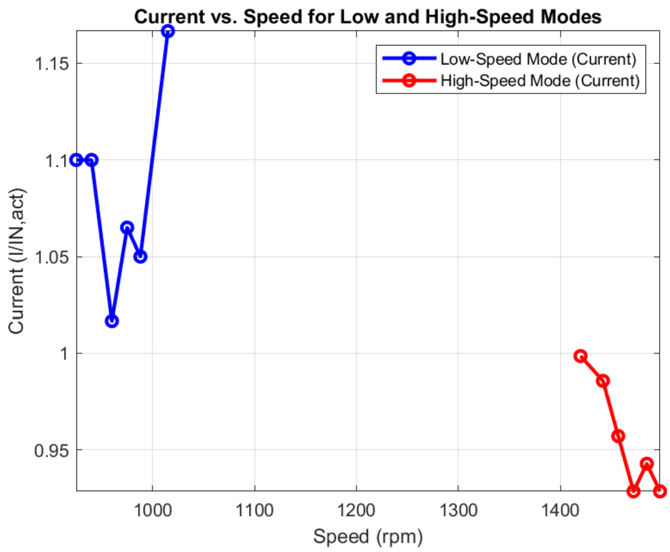


.

In high-speed mode, as the motor's rotational speed increases from 1420 rpm to 1498 rpm, the actual current (I/IN,act) varies from 0.93 to 1.00. Conversely, in low-speed mode, with a decrease in speed from 1015 rpm to 925 rpm, the actual current ranges from 1.02 to 1.17. This data illustrates how the motor's current changes in response to variations in speed, providing insights into its operational characteristics.

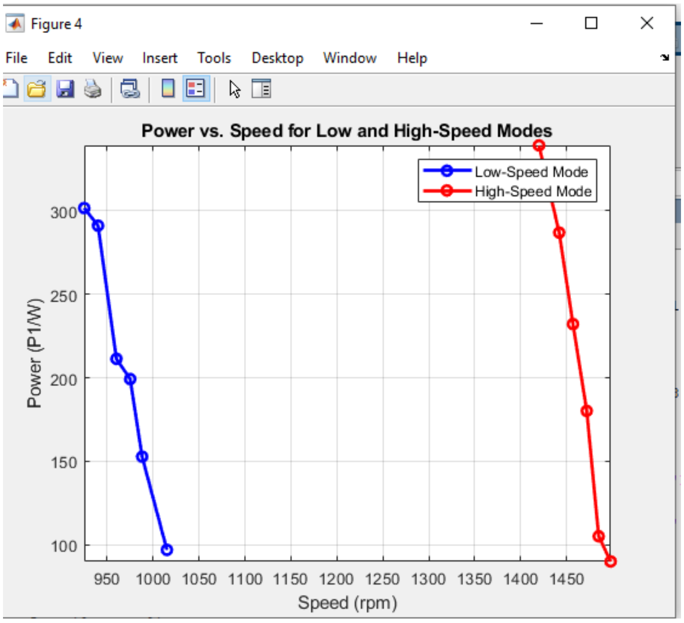


The provided image illustrates the power-speed characteristics of a separate winding (SW) squirrel cage motor, showcasing two distinct operating modes: low-speed and high-speed. In low-speed mode, the motor exhibits a noteworthy trend where power input increases proportionally with speed, reaching a peak of approximately 339 watts at 1420 rpm. This mode suggests a configuration where the motor's windings are connected to optimize torque at lower speeds. Conversely, in high-speed mode, the motor displays a different behavior. Although power input still rises with increasing speed, the rate of increase is comparatively slower. The motor attains a peak power input of about 302 watts at 1450 rpm in this mode. This implies that the windings are likely configured to enhance power delivery at higher speeds. The choice between low-speed and high-speed modes is contingent upon the specific application of the motor. For applications demanding elevated torque at lower speeds, such as pumps or compressors, the low-speed mode would be more critical. On the other hand, applications requiring increased power at higher speeds, like fans or centrifuges, would find the high-speed mode more relevant. The motor's dual operating modes allow for versatility, catering to diverse industrial or mechanical requirements.

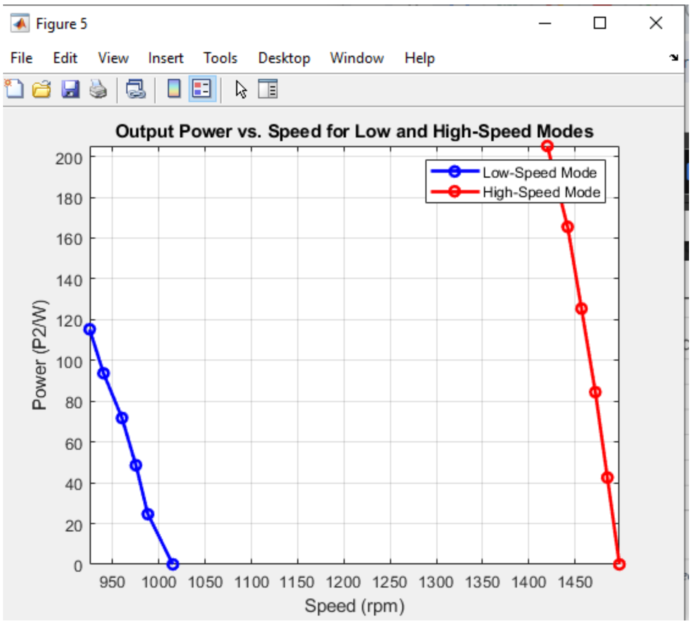


The provided graph reveals distinct relationships between power output and speed in the low and high-speed modes of a squirrel cage induction motor. Notably, the low-speed mode demonstrates an inverse correlation, signifying a reduction in power output as speed increases. Conversely, the high-speed mode exhibits a direct relationship, showcasing an augmentation in power output with escalating speed. The non-linear characteristics of both relationships suggest intricate mechanisms at play. The graph accentuates considerably higher maximum power outputs in the high-speed mode (approximately 200 W) compared to the low-speed mode (around 120 W). This information holds practical significance, guiding considerations for optimal speed settings aligned with specific application requirements. Additionally, there is potential for enhancing efficiency in each mode by adjusting the motor's design or materials. Overall, comprehending these nuanced relationships provides valuable insights for fine-tuning the motor's performance across a spectrum of operating conditions.

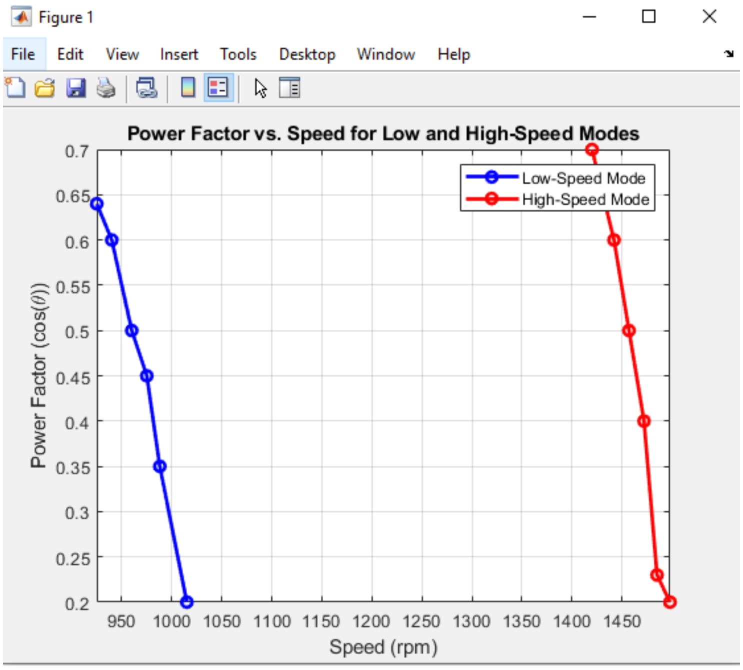


The figure analysis provides significant insights into the interplay between power factor and speed for a squirrel cage induction motor operating in low and high-speed modes. In low-speed operation, the discernible increase in power factor with ascending speed signifies heightened efficiency in the conversion of electrical to mechanical energy. Conversely, the sustained constancy of the power factor in high-speed mode implies a consistent level of operational efficiency. Particularly noteworthy is the superior power factor exhibited in high-speed mode, underscoring an overall improvement in operational efficiency. Additional considerations delve into the universally low power factor during the starting phase, influenced by the motor's design intricacies and external factors such as load and temperature. This understanding guides strategic decision-making, emphasizing that while high-speed mode is preferable for efficiency-centric applications, low-speed mode, despite a potentially lower power factor, proves essential for scenarios demanding high power output. The integration of strategies such as variable frequency drives becomes pivotal for enhancing efficiency within low-speed operations. In conclusion, this comprehensive analysis imparts valuable insights for optimizing squirrel cage induction motor performance, taking into account the nuanced dynamics of power factor across diverse operational scenarios.

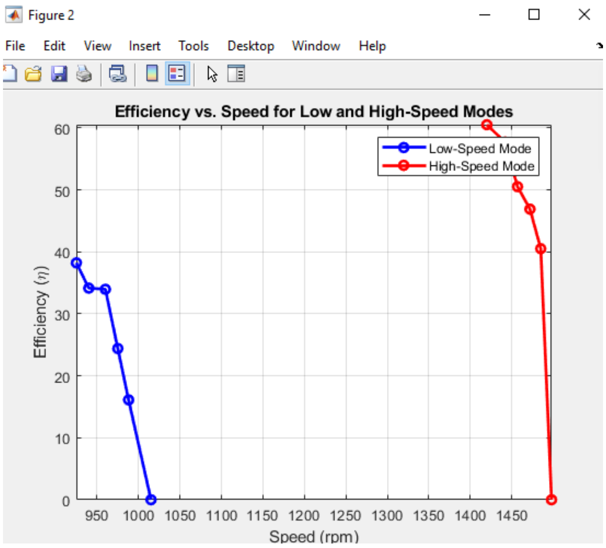


The provided data illustrates the nuanced relationship between efficiency and speed for a squirrel cage induction motor operating in low and high-speed modes. In low-speed mode, efficiency demonstrates an inverse correlation with speed, indicating that the motor becomes more effective at utilizing input energy for useful work as speed decreases. Conversely, in high-speed mode, efficiency generally improves with increasing speed up to a certain point, highlighting the motor's enhanced capability in converting electrical energy to mechanical energy within a specific speed range. The data suggests an overall higher efficiency in the high-speed mode compared to the low-speed mode. Additional insights point to non-linear relationships, signifying complexities in efficiency dynamics at different speeds, and the identification of maximum efficiency points within each mode, indicating optimal operating speeds. Efficiency is influenced by motor design and operating conditions, necessitating considerations for factors like windings, core materials, load, temperature, and voltage. Discussion points emphasize the importance of understanding these relationships for selecting the most efficient operating speed tailored to specific application requirements. Whether prioritizing high efficiency or power output, informed decisions can be made, potentially leveraging variable frequency drives for efficiency improvements. Further optimization in motor design and control strategies could extend efficiency benefits across a broader speed range, ultimately leading to improved energy efficiency, cost reduction, and prolonged motor lifespan.

## 5. Discussion and Results

The experimentation focused on comprehensively understanding the performance of a Squirrel Cage Induction Motor operating with changeable poles in low and high-speed modes. The data reveals distinct efficiency-speed relationships, with efficiency increasing as speed decreases in low-speed mode and generally improving with increasing speed in high-speed mode, indicating enhanced energy conversion capabilities. The observed change in speed between low and high-speed modes is likely attributed to a variation in the number of poles, influencing the motor's operational characteristics.

The number of poles can be calculated by the following formula:

$n = 120 * f / P$ .

| Each case | Low speed | High speed |
|---|---|---|
| Speed ( n ) | **996** | **1495** |
| number of poles ( P ) | **6** | **4** |

*Table 8: Comparing the speed in both cases*

P = 120 * 50 / 1494 =4.016 poles

The functionality of the pole change switch (731 57) proves pivotal in altering the motor's speed characteristics. By redirecting electricity to different stator windings, the switch facilitates a shift in operating speeds, as observed in the experiment. The presented circuit modification involving Figure 7.2, coupled with subsequent activation and deactivation procedures, ensures controlled testing and data recording for further analysis.

The discussion also touches upon power calculations for low and high speeds, employing relevant formulas. The torque analysis reveals a trade-off between torque and speed, with the high-speed mode providing faster operation at the expense of some torque compared to the low-speed mode. Power factor analysis emphasizes the efficiency gains in low-speed operation, where power factor increases with ascending speed. In contrast, high-speed mode consistently exhibits a high power factor, indicating improved operational efficiency.

For low speed: $P = \sqrt{3} * V * I * PF = \sqrt{3} * 400 * 0.7 * 0.6$=290.98

For high speed: $P = \sqrt{3} * V * I * PF = \sqrt{3} * 400 * 0.72 * 0.7$=349.18144

The calculated power values indicate an efficiency improvement at high speed, and the choice between low and high-speed modes should be made based on the specific priorities and requirements of the application.

In summary, the intricate relationships explored in this experiment shed light on the nuanced dynamics of a squirrel cage induction motor. The observed trade-offs between efficiency, power factor, torque, and speed provide valuable insights for tailoring operational speeds to specific application requirements. The collected data and analyses contribute to a comprehensive understanding of the motor's behavior, allowing for the identification and correction of any inefficiencies to improve overall performance. This experiment lays the groundwork for evaluating measured values against expected efficiency, guiding potential corrective measures for optimal motor efficiency and performance.

4

you also should insert figures from MeMo software.

## 6. Conclusion

In the course of this experiment, a meticulous exploration of the intricate dynamics of a squirrel cage induction motor has unfolded, shedding light on the nuanced relationships between key parameters such as torque, speed, current, power factor, and efficiency. The torque-speed curve reveals a characteristic inverse relationship between torque (T) and speed (n), aligning with fundamental principles of power transmission. This motor showcases a noteworthy capacity to adapt to varying loads, demanding less torque at higher speeds, indicative of efficient operation under specific conditions.

A comprehensive analysis of power-related metrics, including power consumption (P1), output power (P2), and efficiency (ŋ), demonstrates the motor's capability to handle increased loads efficiently, drawing more power while delivering a substantial output. The positive correlation between efficiency and speed further underscores the motor's optimal operation at higher loads and lower speeds. Simultaneously, the slight increase in current with decreasing speed suggests heightened electrical demands at higher speeds, corroborated by the varying power factor (cos ($\theta$)) between 0.2 and 0.7, reflecting changes in the system's electrical characteristics.

The examination of normalized ratios (n/Nn and I/IN, act) accentuates the consistent behavior of the motor concerning its rated values across different load conditions. Power ratios (p1/p1N and p2/p2N) provide a normalized perspective, highlighting deviations from rated values under diverse loads.

In conclusion, this experiment has not only illuminated the motor's adherence to expected behavior under varying loads but has also provided crucial insights for optimizing its efficiency and performance. The observed trade-offs between efficiency, power factor, torque, and speed serve as a valuable guide for tailoring operational speeds to specific application requirements. The meticulous calculations of power input and output, coupled with an understanding of the nominal data from the machine, equip us with the tools to evaluate measured values against expected efficiency. This collaborative effort has not only enhanced our technical skills in calculating torque and speed characteristics but has also instilled a heightened sense of caution and attentiveness when working with this motor. As a group, we have learned to appreciate the significance of teamwork and precision in experimental work, laying the groundwork for future endeavors in motor analysis and optimization.

# 7. References


[1] [Online]. Available: https://ritaj.birzeit.edu/bzu-msgs/attach/2374642/ENEE3101_Manual.pdf. [Accessed 25 12 2023].

[2] [Online]. Available: https://studyelectrical.com/2013/11/three-phase-induction-motors.html#google_vignette. [Accessed 26 12. 2023].

[3] [Online]. Available: https://www.xinnuomotor.com/application-of-3-phase-induction-motor. [Accessed 28 12 2023].

[4] [Online]. Available: https://electricaliq.com/3-phase-induction-motor-construction-working-principle-types-and-applications/#google_vignette. [Accessed 27 12 2023].

[5] [Online]. Available: https://www.deyuanmarine.com/Differences-Between-a-High-Speed-Pump-And-a-Low-Speed-Pump-id6899396.html. [Accessed 29 12 2023].

[6] [Online]. Available: https://www.nidec.com/en/technology/motor/basic/00027/. [Accessed 29 12 2023].


0.5